Research Article | Vol. 11, No. 6 / 1 June 2020 / Biomedical Optics Express 2889
Biomedical Optics EXPRESS

Non-contact direct selective laser trabeculoplasty: light propagation analysis

ZACHARY S. SACKS,[1,*] MASHA DOBKIN-BEKMAN,[1] NOA GEFFEN,[2,3] MORDECHAI GOLDENFELD,[4] AND MICHAEL BELKIN[1,5]

[1]BELKIN Laser, Ltd., 13 Gan Raveh, POB 13254, Yavne 8122214, Israel
[2]Sackler Faculty of Medicine, Tel Aviv University, Tel Aviv 6997801, Israel
[3]Department of Ophthalmology, Rabin Medical Center, Petah Tikva 49100, Israel
[4]Goldschleger Eye Institute, Sheba Medical Center, Tel Hashomer 52621, Israel
[5]Goldschleger Eye Research Institute, Tel Aviv University, Tel Hashomer 52621, Israel
[*]zachary@belkin-laser.com

Abstract: Selective laser trabeculoplasty (SLT), used to treat glaucoma and ocular hypertension, requires the use of a gonioscope placed on the cornea to visualize and irradiate the trabecular meshwork (TM). Alternatively, non-contact direct SLT (DSLT) irradiates the TM through the overlying tissues. Here we analyze this innovative procedure using analytical modeling and Monte Carlo simulations to quantify the laser energy reaching the TM through the overlying tissues. Compared with energy launched from the laser, DSLT energy transmission to the TM is 2.8 times less than SLT, which verifies the efficacy of non-contact DSLT given the lowest reported effective SLT energies.

1. Introduction

Glaucoma, a chronic disease that gradually impairs vision and may eventually cause blindness, affects more than 70 million people worldwide and is expected to afflict 112 million by 2040 [1,2]. The only treatable risk factor for progression of this disease is its characteristically high intraocular pressure (IOP). Thus, the primary goal of glaucoma therapy is to lower the IOP, thereby reducing the risk of progressive optic disc degeneration and consequent visual field loss resulting in vision impairment which may culminate in blindness [3,4]. Disease progression can be slowed by medication, laser treatment, or surgery [5]. Topical medications (eye drops), a common first-line treatment, have notoriously poor adherence, with only 23% to 60% of patients consistently using their medications as prescribed over 12 months [6–9]. Recent studies have found laser trabeculoplasty treatment to be superior to drug therapy as a first-line treatment in open angle glaucoma (described below) [10], or when pharmaceutical treatment fails to achieve adequate reduction of IOP [11].

1.1. Conventional glaucoma laser treatments

Glaucoma can be classified into open-angle glaucoma, in which the trabecular meshwork (TM), the entrance of the aqueous humor drainage passageway, is visible, and angle closure categories, in which the drainage through the TM is obstructed by angle narrowing, usually by iris adhesions or anterior bowing of the iris. Each type of glaucoma has multiple possible causes.

Argon laser trabeculoplasty (ALT), an alternative to eye drops, was introduced by Wise and Witter in 1979 [12,13]. In this procedure, laser energy is delivered to the TM, in order to cause a thermally-induced structural changes resulting in IOP reduction. The TM is located in the anterior chamber angle. The anterior chamber angle is formed by the intersection of the cornea and iris edge and extends around the entire circumference. The TM is obscured from normal view by the light-scattering white tissues of the scleral limbus. A typical ALT procedure delivers 50−100 laser shots to the TM. Typically, ALT laser shot parameters are 532 nm (the argon laser

#390849 https://doi.org/10.1364/BOE.390849
Journal © 2020 Received 17 Feb 2020; revised 29 Apr 2020; accepted 30 Apr 2020; published 7 May 2020

Biomedical Optics EXPRESS

at 514 nm has since been replaced by the frequency-doubled Nd:YAG), peak power 0.3−1.0 W, exposure 0.1 s, and spot diameter 50 µm [14]. Long-term ALT follow-up shows that after a few years most patients revert to a higher IOP. Since ALT alters the tissue permanently, it can be carried out only on the untreated TM [15,16]. In an effort to minimize the permanent structural changes resulting from ALT, Latina et al. launched Selective Laser Trabeculoplasty (SLT) in 1998 using a low-energy, nanosecond-pulsed laser [17]. Figure 1(a) depicts standard SLT delivery of the laser beam to the TM using a gonioscope, allowing for visualization and laser targeting of the TM through the cornea.

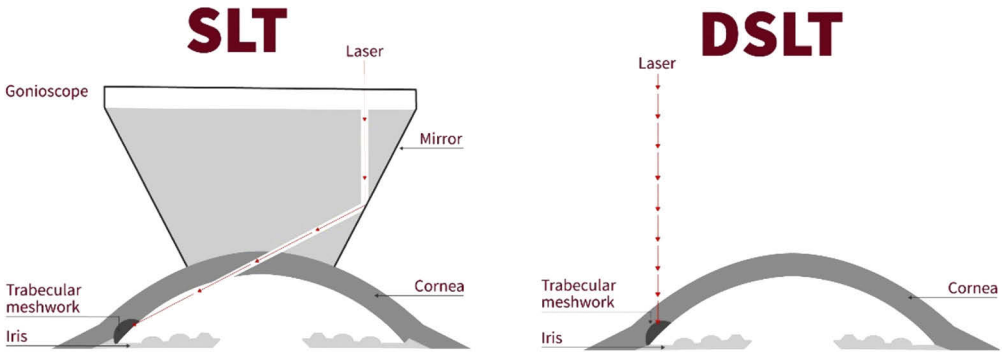

Fig. 1. Laser delivery for SLT (a) and DSLT (b).

The short SLT pulse duration does not allow the heat deposited during the pulse to diffuse from the light-absorbing melanin granules within the cells, thereby reducing collateral damage. SLT uses a frequency-doubled, Q-switched 3 ns, 532 nm Nd:YAG laser with a spot size of 400µm. The energy deposited per laser spot in SLT is about three orders of magnitude less than in ALT. In addition, SLT produces less post-laser inflammation of the anterior chamber than ALT, and it leaves the TM virtually intact, damaging only the endothelial cells which regenerate [18]. Repeat SLT treatments showed that the mean IOP following both initial and repeated SLT procedures had been significantly reduced, meaning that repeat SLT treatments are possible [19–21]. Recent prospective studies in which SLT was used as the primary therapy have shown IOP reductions of about 30% below baseline untreated levels [22].

For standard SLT therapy the surgeon starts by using a laser-shot energy of 0.7–0.8 mJ, with upward or downward energy titration until a bubble forms on the surface of the TM in the aqueous humor, as visualized by a surgical microscope through the gonioscope. The energy level resulting in such bubble formation (the 'champagne level') is called the threshold energy, although there is no proven relationship between the threshold energy and the desired IOP reduction effect. The recommended energy setting for conventional treatment is 0.1 mJ less than the threshold energy [23].

There is considerable clinical variation in how SLT is performed, with no prescribed standard energy, spot number, or extent of lasering on the TM [24] although a recent large clinical study has narrowed the parameters [10]. All existing devices must be operated in combination with a gonioscope lens (Fig. 1(a)), which targets the laser beam through the cornea to the TM treatment zone. Reported side effects with the traditional treatment include a short-term IOP increase, postoperative corneal edema, inflammation, corneal hysteresis, redness, discomfort, and anterior chamber reactions. These side effects originate from the use of the gonioscope because of its contact with and rotation on the cornea, from the passage of the laser beam through the cornea, or both [25]. Moreover, treatments with the existing devices use about 100 manually delivered

Biomedical Optics EXPRESS

single-laser shots, requiring both time and special expertise, which explains why SLT, despite its effectiveness, has not traditionally been offered as a first-line treatment for glaucoma.

1.2. Mechanism of action

The mechanism of action of SLT is not fully understood, although it is believed that it has to do more with cellular and less with mechanical factors [26]. Cvenkel, et al. compared ALT and SLT by applying, in three patients, each treatment on a different part of the same eye, removing the eyes after one to five days, and then examining *ex vivo* [27]. At energy levels above threshold (i.e., higher than in typical treatments), SLT caused some slight damage to the pigmented cells of the TM as shown by light microscopy and transmission electron microscopy. The TM remained intact except for cracks in the corneoscleral sheets and a few endothelial cells with disrupted pigment granules and vacuoles. Again, these effects occurred above accepted treatment energy levels. There is also reported evidence of TM cell division following both ALT and SLT [28]. Alvarado et al. suggested that modulation of aqueous outflow after SLT is caused by macrophages removing debris from the TM [29]. Long-term modification of the TM has not been observed after typical SLT, allowing for repeat treatments [19–21].

The laser-tissue interaction mechanism underlying the absorption of laser energy in SLT is not well understood. Latina et al [17]. theorized that the mechanism involves linear absorption in melanin, but subsequent studies seem to find absorption in melanin less important [30]. Typical laser fluence for a SLT single spot (0.8 mJ, 400 µm, 3 ns) is 1.3 J·cm^{-2} and a peak power of >400 MW·cm^{-2}. These numbers, however, may underestimate the localized peak fluences and powers, since diffuse reflection of the pulse from within the tissue may increase the intensity and fluence close to the surface of the TM [31]. Furthermore, since the laser is a spatially and temporally coherent source, speckle with high peaks can be expected on and within the TM. It would therefore be reasonable to expect that nonlinear absorption processes (including plasma formation) owing to high-peak powers may occur, together with linear absorption [32]. There also exists the possibility of photobiomodulation mechanisms [33]. Recently hyper-reflective particles in the anterior chamber after SLT have been observed using OCT appear to correlate with IOP reduction, implying some sort of explosive laser effect, which the authors postulate as thermally induced [34].

1.3. Direct SLT study

Direct selected laser trabeculoplasty (DSLT) was proposed as a method to eliminate the main disadvantages of SLT, namely the necessity of placing of a gonioscope on the cornea to aim the treatment laser to the TM and the skill required to perform the procedure. It was postulated that illuminating the tissue directly overlying the TM, as shown in Fig. 1(b), would have the same clinical effect as irradiating the TM through a gonioscope. In a comparative study of SLT and DSLT, our group demonstrated their equivalent efficacies but advantageously showed that DSLT was accompanied by fewer complications and less patient discomfort [35]. Note that in this study, the same SLT laser system was used without modifications for both SLT and DSLT.

The success of the DSLT procedure, as reported in that study, was somewhat puzzling given the widespread belief that in SLT the laser energy delivered to the TM must be at the sub-millijoule level (just below the ‘champagne bubble’ threshold) in order to cause an effect. That first study [35] led to many questions about how the laser reaches the TM and reacts with it, since the beam is placed on the perilimbal sclera, a highly scattering tissue located above the TM. Where, for example, should the laser be placed so as to ensure maximum irradiation of the TM? How much energy reaches the TM through the light-scattering limbus? If DSLT is claimed to be a fast non-contact procedure, what design considerations, with the first being safety, must be implemented? Questions were also raised about the possibility that other target tissues, if irradiated, might have a pressure lowering effect.

Biomedical Optics EXPRESS

In this paper we analyze the DSLT procedure [35] and discuss design requirements for an automatic and safe procedure. In Section 2 we describe and analyze the placement of the treatment beam in the original study and its relationship to the TM. In Section 3, using a one-dimensional calculation and then Monte Carlo simulation, we calculate the energy reaching the TM. We conclude that section by comparing the laser energy reaching the TM by the SLT and DSLT procedures, in order to explain their similar efficacies. We conclude this section with a discussion of the relevant design considerations for making the DSLT procedure automatic, with an emphasis on laser safety.

2. DSLT laser spot placement

In the original DSLT study, the doctor placed the 400-μm diameter aiming beam of a typical SLT laser system manually on the sclera so that the beam edge was touching the corneal edge, as shown illustrated for a single spot in Fig. 2 [35]. In this section we analyze this placement with respect to the location of the TM.

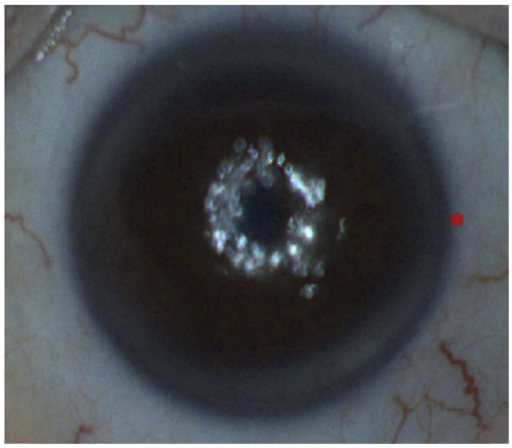

Fig. 2. DSLT beam placement for a single spot. The treatment beam is aligned to the eye by placement of the red aiming beam, as indicated in the figure by a red dot, such that the beam's periphery touches the corneal edge.

To interpret the placement of the laser spot, we start by analyzing the cross-section of the anterior chamber, as shown by optical coherence tomography (OCT) in Fig. 3 as a representative case [36]. The 'Appearance' band at the top of the figure indicates how the eye appears under white light illumination: from the white sclera, through the greyish limbus, to the colored iris seen through the transparent cornea. Of particular relevance is the white border, whose location is described below. Note that the TM is located mainly behind the white and grey portions of the limbus.

The TM starts in the angle vertex (AV) of the iridocorneal angle and extends upwards on the angle. The obvious visible external 'landmark' of the DSLT procedure is the white border of the sclera. The standard measure of this white border is the corneal 'white-to-white diameter' (D_{WTW}) measured by visual inspection using calipers, the extent on one side indicated by WB in Fig. 3 [37].

Although this measurement depends on human judgment, repeatability of about 100 μm has been demonstrated [38]. Another relevant measure of the eye is the angle-to-angle diameter (D_{ATA}), as the AV is the approximate starting point of the TM. D_{ATA} has been measured by using OCT of the entire anterior chamber to locate the AV on both sides and measuring the diameter between these two points in the image [39]. Thus, since the TM starts at the AV, the location of

Biomedical Optics EXPRESS

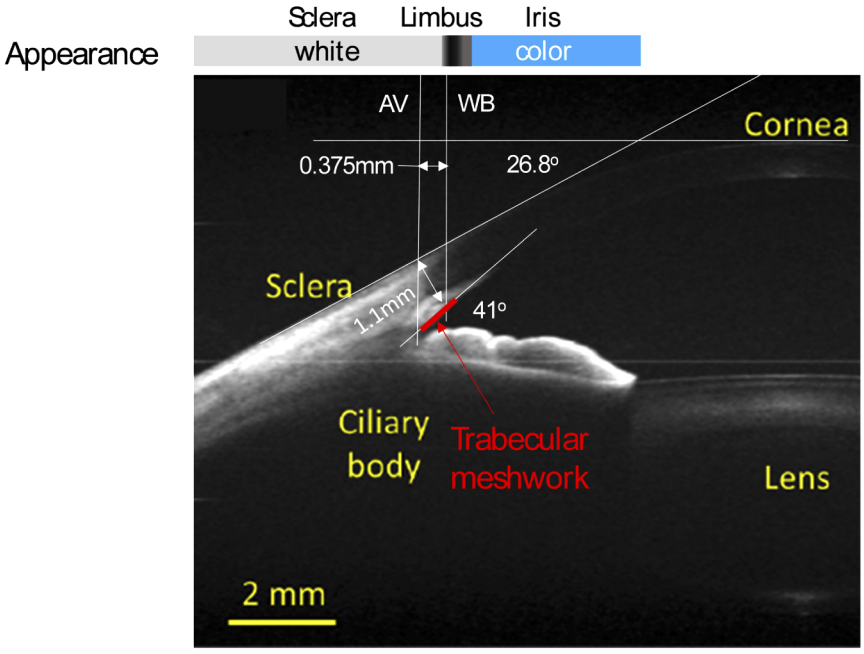

Fig. 3. OCT image [36] of the eye with measurements. The bar at the top shows the appearance of the eye as seen with visible light. The extent of the TM as seen in this cross section is 0.825 mm, as explained below. Angles were obtained by measuring the tangent lines shown in the image with the scale bar the same in both horizontal and vertical directions. AV, angle vertex; WB, white border.

the TM in relation to the white border of the sclera can be determined assuming that the eye is symmetric across its center.

D_{ATA} and D_{WTW} have been previously reported [38,39]. The data from Goldsmith, et al [39]., obtained under visible light, are used here. The average D_{ATA} is 12.53 mm (0.47 mm standard deviation; SD) and the average D_{WTW} is 11.78 mm (0.57 mm SD), meaning that the distance between the white border and the AV is 0.375 mm on average (half the difference of the diameters), which is approximately the diameter of the treatment beam. This interesting result shows that the placement of the 0.4 mm laser spot is directly above the TM, thus minimizing the distance of the laser delivery point to the TM on average.

Since the TM is at an angle with respect to the axis of the eye, we next derive, from the position of the AV, the extent of the TM from the white limbus edge. Figure 4 shows a geometric model of the anterior angle. The average length of the TM (red line) has been reported as 700 ± 200 µm (mean $\pm$ 2 SD) measured histologically [40] and 825 ± 182 µm (mean $\pm$ SD) measured on live eyes by OCT As seen in Fig. 4, it would appear that some of the TM extends 250 µm beyond the white edge into the gray region of the limbus.

Since the beam is incident at an angle, refraction would be expected if the spot is placed directly on the edge of the sclera. Thus, for example, taking an incident angle of 26.8° and assuming the tissue index is similar to that of water ($n \sim 1.33$), the beam deflection would be approximately 130 µm through 1.1 mm of tissue—a minor effect given natural biological variations. We conclude that if the edge of the treatment beam is placed such that the periphery touches the white limbus border, the treatment beam will be positioned directly over the TM.

Biomedical Optics EXPRESS

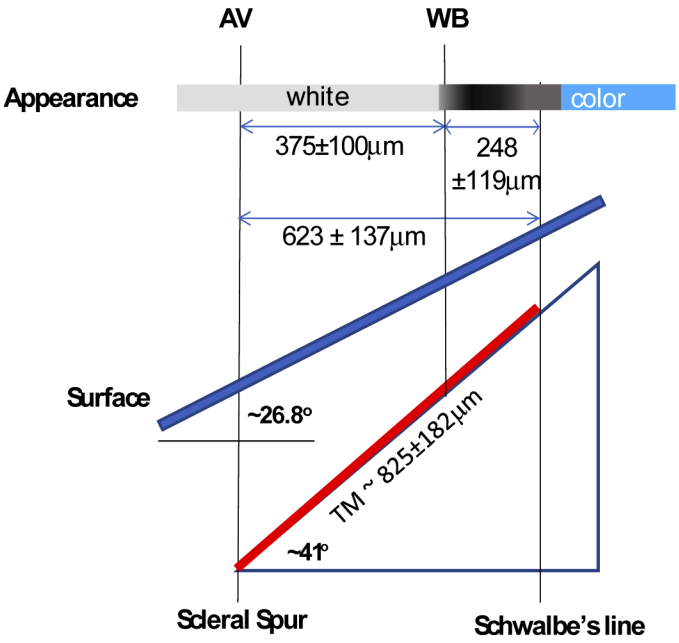

Fig. 4. Geometric model of the anterior chamber angle.

3. Energy transfer to the trabecular meshwork

Although the original DSLT study [35] targeted the TM by placing the laser on the perilimbal sclera (a highly scattering tissue), the reduction in IOP was equivalent to that obtained by standard SLT, where the laser is directly placed on the TM by delivery through the cornea. The literature contains no conclusive SLT dose-response study of the laser energy required to produce the maximal IOP reduction. In one SLT study, an average pressure-lowering effect of 20% below baseline pressure was reported after laser treatment performed below the 'champagne bubble' threshold, i.e., at a fixed energy of 0.4 mJ [23]. In another study, 0.3 mJ was found to be effective [41]. It has been hypothesized that microbubbles, which form at fluences less than champagne bubbles, cause cell death and the increase in aqueous outflow [42]. It should be noted that the energy levels stated for the foregoing procedures refer to the energy launched from the device, not the energy reaching the TM. In the following DSLT analysis, we provide quantitative calculations of the amount of light reaching the TM through the light-scattering tissue, and then compare the result with the energy reaching the TM in SLT using 0.3 mJ, the lowest reported effective SLT dose after allowing for losses and geometric effects.

In the absence of published data on optical properties of the limbus, we approximate them by using the average of the optical properties of the cornea and the sclera, since the limbus is the transition region between these tissues [43]. Reports on optical properties of the sclera [44,45] indicate that this tissue reflects about 60% of 532-nm light, and transmits about 10% of the light through its full (0.8 mm) thickness as measured with integrating spheres. These values do not include effects from overlying tissues such as conjunctiva. In addition, the effective spot size increases through the tissue owing to scattering upon propagation [46–49].

3.1. One-dimensional estimation

We assume that the limbus is half cornea, assumed to be transparent, and half sclera. Through a full thickness of 0.8 mm sclera, transmission is 10% at 532 nm [44]. Using Beer's Law [31], the

Biomedical Optics EXPRESS

attenuation coefficient is found to be 2.88/mm. If the effective thickness of the equivalent limbus tissue is 0.4 mm sclera, about *exp(-2.88/mm · 0.4mm)* ~ 32% of the light is transmitted through the limbus. By this approximation, about one-third of the incident DSLT laser energy would reach the TM.

The above calculation does not include the geometric effects of beam propagation through the tissue, such as spot size enlargement, which would decrease the fluence reaching the TM. These effects are modeled in the next section and then compared to the above calculation.

3.2. Monte Carlo simulation

A freeware Monte Carlo propagation code, MCmatlab [50], was used to model the propagation of light through the limbus. The code uses the radiative transport equation to simulate light propagating through geometries that are specified in three dimensions by discretizing the domain into rectangular elements called cuboids [31]. Each material is specified by its refractive index n, absorption μ_a, scattering μ_s, and Henyey-Greenstein scattering anisotropy factor g. The code calculates the accumulated absorbed photon energy density (energy/volume) and fluence (energy/area) in each cubiod, as well as the far-field radiative flux as a function of the solid angle. Since photons can enter each cuboid from multiple directions, fluences greater than the launched laser fluence can be achieved owing to the multi-directional scattering.

To specify the tissue properties, we needed to fit the Monte Carlo simulation to existing data based on integrating sphere measurements: total reflection R and total transmission T of the tissue. Using the far-field radiative flux from the simulation, R and T represent the total energy within their respective hemispheres. Absorption A is calculated as the total absorbed energy within the tissue, such that $R + T + A = 100\%$ [31]. In these MCmatlab simulations, light was collected only through the top and the bottom surfaces of the tissue slab so that the reported integrated sphere measurements could be more accurately simulated. This means that light may be trapped inside the tissue and emerge from the sides of the simulation boundaries.

3.2.1. Scleral tissue parameters

We used the range of scattering parameters reported by Bashkatov et al [45]. in the Monte Carlo simulation to obtain the R, T, and A parameters taken from Vogel et al [44]. The sclera model used is shown in Fig. 5. Table 1 and Table 2 show the resulting scattering parameters and the resulting simulated integrated tissue parameters, respectively.

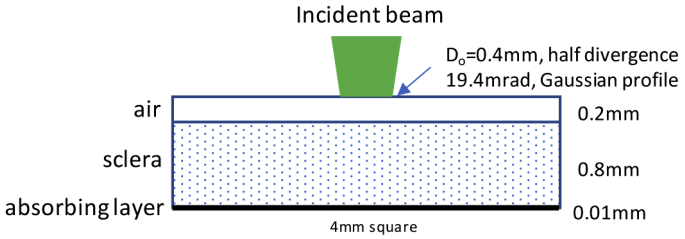

Fig. 5. Geometry for determining sclera scattering coefficients. Cuboid size is 0.01mm on each side.. (Typical sclera thickness 0.8mm [44], an arbitrary air gap of 0.2mm to visualize reflection, and a single cuboid thick absorbing layer of 0.01mm were modeled.)

3.2.2. Sclera spot size calculations

The spot size of the emergent beam was calculated through full-thickness sclera to place an upper bound worst-case scenario on delivery of laser energy to the TM. The spot size and energy were obtained by placing a very highly absorbing single plane of cuboids ($\mu_a = 10^8$ cm^{-1}) on the

Biomedical Optics EXPRESS

Table 1. Scattering Parameters for Human Sclera

Parameter	Symbol	Unit	Reported [45]	Simulated Fit
Absorption	μ_a	cm^{-1}	1–2	1
Scattering	μ_s	cm^{-1}	170–215	213
Anisotropy	g		0.65–0.73	0.64

Table 2. Integrated Tissue Parameters (0.8 mm thickness at 532 nm)

Parameter	Symbol	Reported [44]	Simulated Fit
Total absorption	A	25%	26%
Total transmission	T	8–20%	18%
Total reflection	R	55–70%	56%

posterior sclera surface and plotting the absorbed photon density, normalized such that the total normalized photon density was equal to the total transmission T calculated from a simulation without the absorbing layer.

The size of the transmitted spot through full-thickness sclera was calculated from launching a standard SLT-type beam of spot size 400 μm ($1/e^2$ full width) and half-angle divergence of 19.4 mrad. Figure 6 depicts the normalized fluences on a linear and a log scale. On the linear scale, the incident beam can be seen at the top, impinging on the tissue 0.2 mm below the top of the simulation domain. The log plot shows the extent of scattering. The scattering coefficient provides an expected scattering length value of 52 µm, meaning that on direct transmission through 0.8-mm-thick sclera a photon is expected to be scattered about 16 times. Figure 6(b) qualitatively shows that the beam is highly scattered in the tissue, with an emergent spot size much larger than the incident beam.

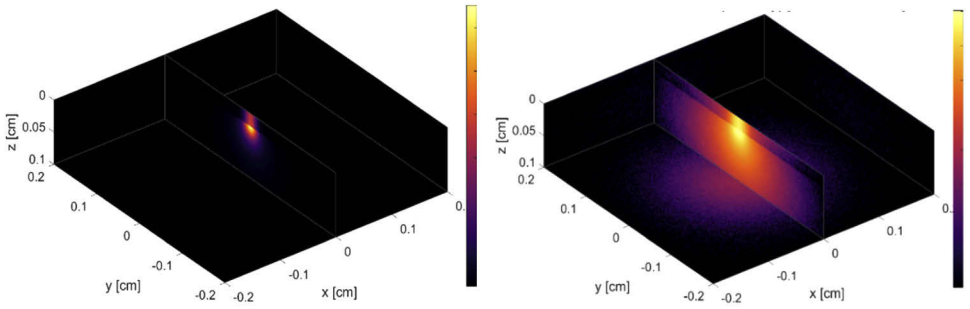

(a) Linear scale (b) Log scale

Fig. 6. MCMatlab normalized fluence rate resultsfor full-thickness sclera. (Simulated 20×10^6 photons.)

Figure 7(a) shows a line-out of the intensity distributions at the launch point and at the back surface of the sclera. The peak intensity at the posterior surface decreases to less than 1% of the incident beam. Figure 7(b) shows that the spot size, as defined by 86.5% enclosed energy diameter is consistent with Gaussian beams, and that it increases from 0.4 mm to 1.94 mm, which is qualitatively in agreement with previous spot size measurements through sclera at longer wavelengths [46].

Biomedical Optics EXPRESS

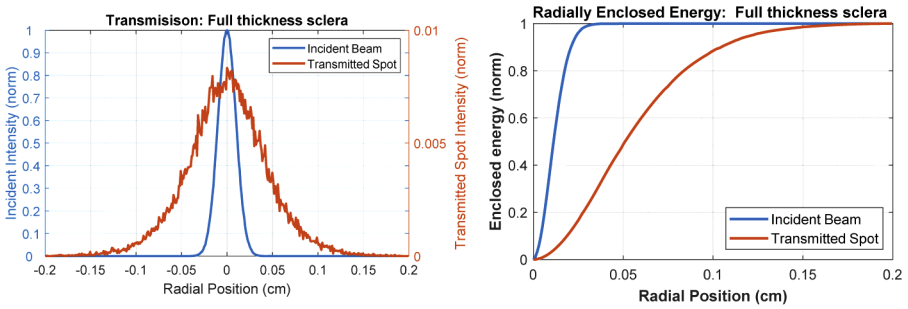

Fig. 7. MCMatlab simulation result for full-thickness sclera. (Simulated 20×10^6 photons.) Radially Enclosed Energy is calculated by integrating the energy about the center of the incident beam.

3.3. Limbus modeling

In this section, laser beam propagation is modeled using the scattering parameters obtained in Section 3.2.1.

3.3.1. Metrics

The following three metrics are defined for analyzing light transmission through tissue:

1) Total transmission: the total integrated energy arriving at the posterior surface of the tissue.

2) Peak transmission: ratio of the maximum transmitted incident fluence on the posterior surface of the tissue to the maximum fluence on the anterior surface of the tissue.

3) Limbus transmission: the integrated energy arriving at the 0.4 mm × 0.825 mm ellipse centered on the peak transmission location at the posterior surface of the sclera, which simulates the TM. (Note that 0.4 mm corresponds to the incident beam width and 0.825 is the average reported width of the TM.)

3.3.2. Limbus structure

The representative limbus shown in Fig. 3 was modeled using the geometry depicted in Fig. 8 and the tissue properties recorded in Table 3, where the limbal sclera tissue was modeled assuming that the scattering coefficients were the average of those in the cornea and those obtained previously in the sclera. Figure 8 shows the incident beam profile in the top left corner, the transmitted spot in the bottom right corner, and a cross section of the simulation at the top right corner. Note that most of the scattering occurs in the first layer of the limbus.

Table 3. Tissue Properties

Parameter	Unit	Air	Sclera	Limbal Sclera	Cornea
n		1	1.42	1.42	1.42
μ_a	cm^{-1}	10^{-8}	1	0.5	10^{-8}
μ_s	cm^{-1}	10^{-8}	213	213/2	10^{-8}
g		1	0.64	(1 + 0.64) / 2	1

Normalized line-out plots of the incident beam and the posterior surface spot are shown in Fig. 9. Limbus transmission was about 11.2%, which is equivalent to the energy of the incident beam reaching the posterior surface of the limbus. Peak transmission through the tissue was

Biomedical Optics EXPRESS

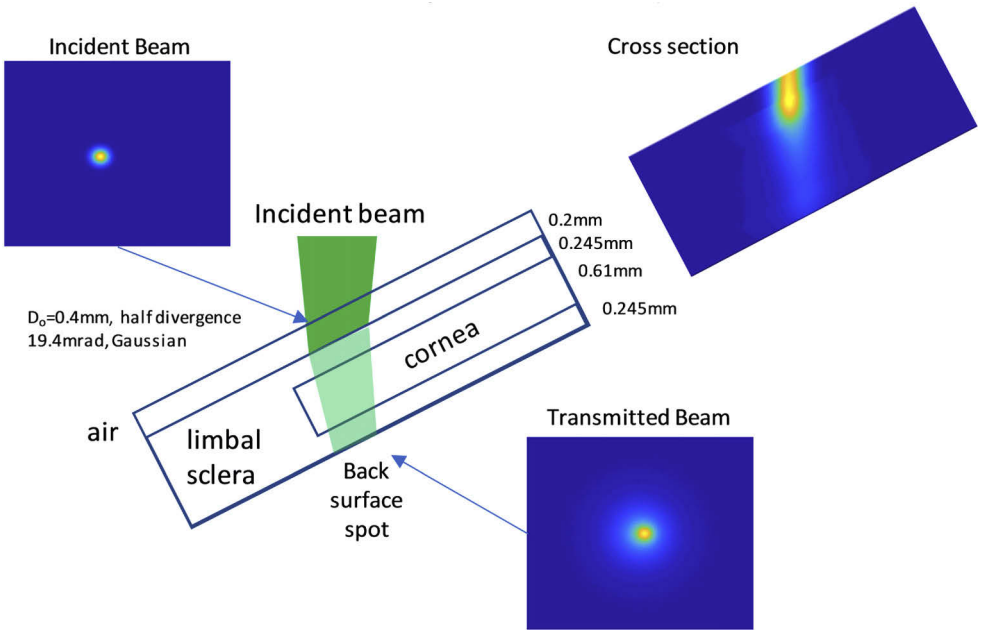

Fig. 8. Simulated limbus geometry and results. Fluence plots are on a linear scale with color scale normalized in each plot. (Limbus geometry is from Fig. 3 measurements.)

6.6%. Total transmission to the posterior surface of the tissue was 45.3%, which is similar to the 32% recorded in Section 2.

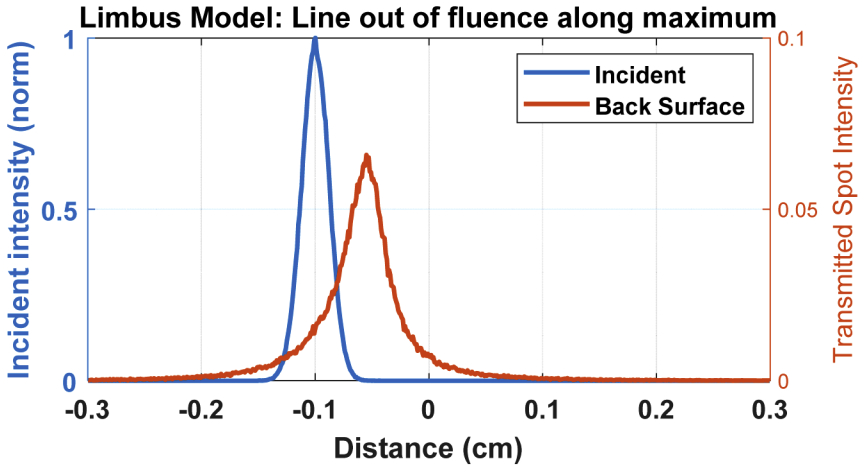

Fig. 9. Normalized fluences of the incident and transmitted beams (top) with line-out normalized to the peak incident beam (right). The shift in the peak beam is due to refraction.

4. Discussion

Using DSLT laser spot placement, the Monte Carlo simulation yielded a peak transmission of 6.6% and a limbus transmission of 11.2% to the TM. Further increase in transmission to the TM may be expected if the laser spot is moved on the limbus towards the pupil as scattering is

Biomedical Optics EXPRESS

expected to decrease in this direction due to the transition of highly scattering scleral to highly transmission corneal tissue [43]. In the following calculation we compare the DSLT and the SLT results.

Figure 10 presents a comparison of the delivery of the DSLT beam and the SLT beam to the TM. The SLT beam approximately bisects the anterior chamber angle, so that in this example the laser impinges on the TM at an angle of about 20.5°. Assuming a diameter beam of 400 µm, the size of the beam on the TM surface would be 1140 µm. Using the limbus transmission metric defined previously, the SLT beam on the TM would be about 1.6 times larger than the TM itself, meaning that energy is lost since it overfills the TM. Examination of SLT images obtained with the aiming beam reveals significant scattering and beam distortion, estimated at a 2× loss including absorption. Thus, SLT energy transmitted to the TM would be 1/2/1.6 ~ 36%. Given that the minimal proven dose of SLT energy effective for IOP reduction is 0.3−0.4 mJ (0.2 mJ appears to have been used in at least part of the treatments [51,52]), as measured in air at the device exit before it enters the gonioscope [23,41], only (0.3−0.4 mJ)×0.36 = 0.09−0.125 mJ of the energy is delivered to the TM. This energy represents the upper bound on a minimal effective dose. As simulated in the previous section, limbus transmission for DSLT is 11.2%. Thus, in order to obtain 0.09−0.125 mJ on the TM, 0.82−1.1 mJ of DSLT energy is required to deliver the 0.3−0.4 mJ SLT dose. The calculation is summarized in Table 4. The original DSLT study used 0.8 mJ; this would be equivalent to 0.3 mJ of SLT, which would seem probable for pressure reduction given the results of the 0.3-mJ study [41].

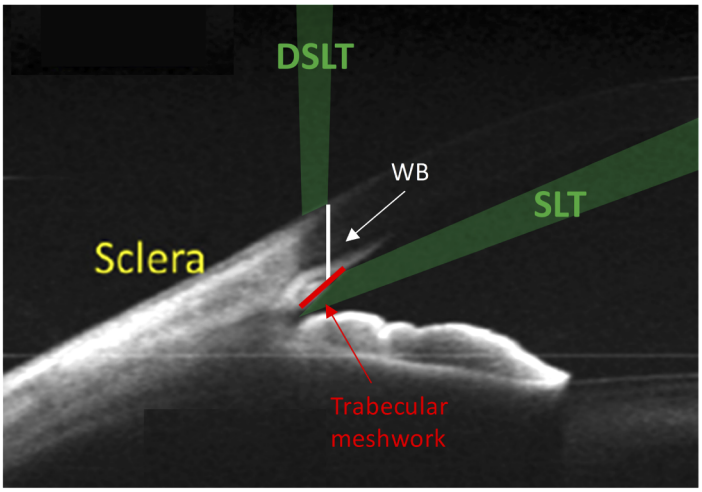

Fig. 10. DSLT and SLT beam delivered to the TM [36].

Table 4. Comparison of SLT and DSLT transmission to TM

Procedure	Parameter	Value
SLT	SLT energy in air (lowest reported effective dose [23])	0.3 mJ
	Transmission due to spot size elongation on TM	63%
	Transmission due to scattering, absorption, and distortion on delivery	50%
	Energy delivered to the TM	0.09 mJ
DSLT	Transmission to TM (Monte Carlo simulation)	11.2%
	DSLT energy in air required to obtain 0.09 mJ on the TM (0.3 mJ SLT dose)	0.8 mJ
DSLT vs. SLT	Increase in DSLT energy over SLT to achieve same delivered energy on the TM	×2.8

Biomedical Optics EXPRESS

DSLT is expected to be as effective as SLT in lowering IOP in all types of glaucoma, including angle closure glaucoma (ACG). In ACG the iris bows forward towards the TM or cornea obstructing fluid drainage through the TM. Direct visualization of the TM with a gonioscope is obstructed and standard SLT laser delivery is not possible. Patients with incomplete ACG have been successfully treated with SLT in regions of the eye where the TM was still visible [53–59]. As SLT has been shown to be effective in lowering IOP in ACG, DSLT is expected to provide a similar pressure lowering result to SLT with the possibility of increased effectiveness as even gonioscopically obscured portions of the TM may be irradiated without a gonioscope, as shown in Fig. 10.

There is a worldwide need to increase the adoption of laser trabeculoplasty as a first-line treatment for patients with open angle glaucoma and ocular hypertension, as SLT has been shown to be efficient and cost effective [10]. Conventional SLT requires a gonioscopy lens to visualize the TM and to aim the laser [60], which requires a high level of skill obtained by training and experience [61,62], and, as such, only 25% of general ophthalmologists offer SLT to their patients [63]. Automation of SLT would make it more accessible to patients, since in addition to highly trained practitioners, the DSLT procedure could be performed by general ophthalmologists and other eye-care providers. In the envisioned non-contact DSLT procedure the patient's head rests on the device, which then automatically determines the laser treatment target. The operator approves and, if necessary, adjusts the target. The laser is then fired to complete the treatment while eye-tracking algorithms keep the laser on target even if the eye moves. The laser treatment itself is intended to take about a second, thus having the added benefit of increasing patient comfort and stability. An additional advantage is that the device does not touch the patient's eye, thus further increasing patient comfort and decreasing side effects associated with the gonioscope laser delivery in conventional SLT procedures. Although standard SLT lasers are reported to operate up to 1 Hz, lasers with higher repetition rates can be made. High-speed laser beam-steering is a mature technology that is commonly used in laser material processing and can move laser spots in milliseconds or less. It should therefore be feasible to automate the DSLT procedure to deliver about 100 laser spots to the TM in a few seconds or less. It will be noted that one difference between SLT and DSLT is that no direct visualization of the TM occurs during DSLT laser delivery: in SLT the TM is visualized with a gonioscope before and after the laser is fired allowing the operator to make adjustments during the procedure.

For SLT a Class 3b laser is used, meaning that direct exposure of the retina to it may cause permanent injury. Calculations conforming with IEC 60825-1:2014 Ed 3 [64] show that a nanosecond laser with a 2 mJ, 532 nm, 400 μm diameter spot is about 1000× above the maximum permissible exposure (MPE) for retina and about at the MPE for skin, which is typically used for all tissues except for retina. No permanent damage is expected on the sclera, limbus, or iris, as the MPE includes a significant margin of safety from permanent damage. As permanent laser modifications require energy above a certain threshold (MPE), no significant difference is expected in undesired consequences between SLT and DSLT as both are at or below the MPE. Given the relation of treatment energy to MPE, no histological studies to evaluate laser induced tissue changes are currently planned, nor have the Institutional Review Boards (IRBs) required them at future clinical sites. (See below for a discussion of the clinical trials.)

When using a non-contact device where the eye is free to move, it is imperative that the device can safely place the laser spot on the correct target location, and not through the pupil to the retina. The system response time can then be calculated by the time taken for the eye to move such that the laser delivery location moves from the typical target location (the white boundary of the sclera) to the edge of the pupil. The fastest motion of the eye is a saccade, which is an involuntary motion. During a saccade the eye can move at speeds of 170 mm/s, which is approximately 1 mm in 5 ms on the surface of the eye [65].

Biomedical Optics EXPRESS

Assuming that the DSLT beam is to be placed such that its periphery touches the white boundary of the sclera, the DSLT target would be a ring about 11.1 mm in diameter, including 3 SDs of the D_{WTW} measurements [39]. For the purpose of this calculation, we assume that the maximum diameter of a contracted pupil is 4 mm [66]. Thus, the beam would have to travel about 3.6 mm in order for its periphery to touch the edge of the pupil. This distance might be less, since the pupil is not necessarily centered in the limbus, the laser spot may extend beyond the 400-µm diameter, and a smaller limbus size should be used to include more of the population. Given these considerations, the system's response time (the time between image exposure and laser fire) should be less than 15 ms to ensure that the laser does not pass through the pupil and damage the retina. Stabilization of the eye can be assisted by providing a fixation target for the patient. As an example for feasibility, refractive eye surgery uses a fixation target with eye tracking at 60 Hz for laser beam placement [67].

BELKIN Laser has constructed a prototype DSLT device, utilizing off-the-shelf components and taking account of the design considerations discussed. Our device, without having direct contact with the eye, automatically delivers 100 laser shots in about one second. The main components of the device include a camera (few ms exposure and data transfer time), high speed galvo scanner mirrors (sub millisecond positioning time), a laser (sub ms response time), and a controller. Before each laser shot the device uses active eye tracking to update the laser targeting, such that the total time from the start of image acquisition to laser delivery is less than 15 ms. A similar non-contact concept using eye tracking an automatic laser targeting has been demonstrated for retinal surgery [68].

5. Conclusions

The DSLT clinical experiment performed by our group and published in 2017 [35] was analyzed here for laser spot placement and laser fluence reaching the TM. By positioning the laser beam on the sclera such that its periphery touched the white boundary, the laser spot is placed directly over the TM, thus minimizing the length of its path to the TM, and hence minimizing its energy loss due to scattering and absorption. The energy reaching the TM during DSLT was calculated to be about 11% of the discharged energy, as compared to about 32% for SLT, noting that energy measurements were taken in air at the device's output. Thus, when comparing the energy levels of SLT to DSLT, a factor of 2.8 should be used. SLT treatment of 0.3 mJ (the lowest reported value yielding IOP reduction) [23] would be equivalent to 0.8 mJ of DSLT. In other words, the use of 0.8 mJ our 2017 DSLT clinical study [35] was equivalent to an SLT treatment of 0.3 mJ, which may explain why DSLT was effective in lowering IOP in that study. Increasing DSLT energy will be the subject of future clinical work.

Funding

Horizon 2020 Framework Programme (No. 720274).

Acknowledgments

The authors thank Anders Kragh Hansen, Department of Photonics Engineering, Technical University of Denmark, for assistance and modifications to MCmatlab. Writing assistance was provided by Shirley Smith.

Disclosures

ZS: BELKIN Laser Ltd (ICP). MDB: BELKIN Laser Ltd (EP). NG: BELKIN Laser Ltd (C). MG: BELKIN Laser (CP). MB: BELKIN Laser Ltd, Tel Aviv University (ICP)

Biomedical Optics EXPRESS

References

1. Y.-C. Tham, X. Li, T. Y. Wong, H. A. Quigley, T. Aung, and C.-Y. Cheng, "Global prevalence of glaucoma and projections of glaucoma burden through 2040: a systematic review and meta-analysis," Ophthalmology **121**(11), 2081–2090 (2014).
2. H. A. Quigley and A. T. Broman, "The number of people with glaucoma worldwide in 2010 and 2020," Br. J. Ophthalmol. **90**(3), 262–267 (2006).
3. P. C. Maier, J. Funk, G. Schwarzer, G. Antes, and Y. T. Falck-Ytter, "Treatment of ocular hypertension and open angle glaucoma: meta-analysis of randomised controlled trials," BMJ **331**(7509), 134 (2005).
4. L. Hyman, A. Heijl, M. C. Leske, B. Bengtsson, and Z. Yang, "Natural History of Intraocular Pressure in the Early Manifest Glaucoma Trial: A 6-Year Follow-up," Arch. Ophthalmol. **128**(5), 601–607 (2010).
5. P. J. Pisella, "Prevalence of ocular symptoms and signs with preserved and preservative free glaucoma medication," Br. J. Ophthalmol. **86**(4), 418–423 (2002).
6. J. P. Jones, D. S. Fong, E. N. Fang, C. A. Mesirov, and V. Patel, "Characterization of Glaucoma Medication Adherence in Kaiser Permanente Southern California," https://www.ingentaconnect.com/content/wk/jglau/2016/00000025/00000001/art00008.
7. M. Feehan, M. A. Munger, D. K. Cooper, K. T. Hess, R. Durante, G. J. Jones, J. Montuoro, M. A. Morrison, D. Clegg, A. S. Crandall, and M. M. DeAngelis, "Adherence to Glaucoma Medications Over 12 Months in Two US Community Pharmacy Chains," J. Clin. Med. **5**(9), 79 (2016).
8. D. T. Quek, G.-T. Ong, S. A. Perera, E. L. Lamoureux, and T. Aung, "Persistence of patients receiving topical glaucoma monotherapy in an Asian population," Arch. Ophthalmol. **129**(5), 643–648 (2011).
9. N. S. Ting, J. F. Li Yim, and J. Y. Ng, "Different strategies and cost-effectiveness in the treatment of primary open angle glaucoma," Clinicoecon Outcomes Res **6**, 523–530 (2014).
10. G. Gazzard, E. Konstantakopoulou, D. Garway-Heath, A. Garg, V. Vickerstaff, R. Hunter, G. Ambler, C. Bunce, R. Wormald, N. Nathwani, K. Barton, G. Rubin, M. Buszewicz, G. Ambler, K. Barton, R. Bourne, D. Broadway, C. Bunce, M. Buszewicz, A. Davis, A. Garg, D. Garway-Heath, G. Gazzard, R. Hunter, H. Jayaram, Y. Jiang, E. Konstantakopoulou, S. Lim, J. Liput, T. Manners, S. Morris, N. Nathwani, G. Rubin, N. Strouthidis, V. Vickerstaff, S. Wilson, R. Wormald, and H. Zhu, "Selective laser trabeculoplasty versus eye drops for first-line treatment of ocular hypertension and glaucoma (LiGHT): a multicentre randomised controlled trial," Lancet **393**(10180), 1505–1516 (2019).
11. J. Lusthaus and I. Goldberg, "Current management of glaucoma," Med. J. Aust. **210**(4), 180–187 (2019).
12. J. B. Wise and S. L. Witter, "Argon laser therapy for open-angle glaucoma: a pilot study," Arch. Ophthalmol. **97**(2), 319–322 (1979).
13. U. Ticho and H. Zauberman, "Argon laser application to the angle structures in the glaucomas," Arch. Ophthalmol. **94**(1), 61–64 (1976).
14. S. L. Groth, E. Albeiruti, M. Nunez, R. Fajardo, L. Sharpsten, N. Loewen, J. S. Schuman, and J. L. Goldberg, "SALT Trial: Steroids after Laser Trabeculoplasty," Ophthalmology **126**(11), 1511–1516 (2019).
15. W. G. Hodge, "Baseline IOP predicts selective laser trabeculoplasty success at 1 year post-treatment: results from a randomised clinical trial," Br. J. Ophthalmol. **89**(9), 1157–1160 (2005).
16. I. McIlraith, M. Strasfeld, G. Coley, and C. M. L. Hutnik, "Selective laser trabeculoplasty as initial and adjunctive treatment for open-angle glaucoma," Am. J. Ophthalmol. **142**(2), 364 (2006).
17. M. A. Latina, S. A. Sibayan, D. H. Shin, R. J. Noecker, and G. Marcellino, "Q-switched 532-nm Nd:YAG laser trabeculoplasty (selective laser trabeculoplasty): A multicenter, pilot, clinical study," Ophthalmology **105**(11), 2082–2090 (1998).
18. J. M. Martinez-de-la-Casa, J. Garcia-Feijoo, A. Castillo, M. Matilla, J. M. Macias, J. M. Benitez-del-Castillo, and J. Garcia-Sanchez, "Selective vs argon laser trabeculoplasty: hypotensive efficacy, anterior chamber inflammation, and postoperative pain," Eye **18**(5), 498–502 (2004).
19. B. A. Francis, N. Loewen, B. Hong, L. Dustin, K. Kaplowitz, R. Kinast, J. Bacharach, S. Radhakrishnan, A. Iwach, L. Rudavska, P. Ichhpujani, and L. J. Katz, "Repeatability of selective laser trabeculoplasty for open-angle glaucoma," BMC Ophthalmol. **16**(1), 128 (2016).
20. A. S. Khouri, H. B. Lari, T. L. Berezina, B. Maltzman, and R. D. Fechtner, "Long Term Efficacy of Repeat Selective Laser Trabeculoplasty," J Ophthalmic Vis Res **9**(4), 444–448 (2014).
21. J. Polat, L. Grantham, K. Mitchell, and T. Realini, "Repeatability of selective laser trabeculoplasty," Br. J. Ophthalmol. **100**(10), 1437–1441 (2016).
22. L. J. Katz, W. C. Steinmann, A. Kabir, J. Molineaux, S. S. Wizov, and G. Marcellino, "Selective laser trabeculoplasty versus medical therapy as initial treatment of glaucoma: a prospective, randomized trial," J Glaucoma **21**(7), 460–468 (2012).
23. H. Y. Zhang, Y. J. Qin, Y. F. Yang, J. G. Xu, and M. B. Yu, "Intraocular Pressure-Lowering Potential of Subthreshold Selective Laser Trabeculoplasty in Patients with Primary Open-Angle Glaucoma," J. Ophthalmol. **2016**, 1–6 (2016).
24. D. B. Kagan, N. S. Gorfinkel, and C. M. Hutnik, "Mechanisms of selective laser trabeculoplasty: a review," Clin. Exp. Ophthalmol. **42**(7), 675–681 (2014).
25. Y. Zhou and A. A. Aref, "A Review of Selective Laser Trabeculoplasty: Recent Findings and Current Perspectives," Ophthalmol Ther **6**(1), 19–32 (2017).
26. A. Garg and G. Gazzard, "Selective laser trabeculoplasty: past, present, and future," Eye **32**(5), 863–876 (2018).

Biomedical Optics EXPRESS

27. B. Cvenkel, A. Hvala, B. Drnovšek-Olup, and N. Gale, "Acute ultrastructural changes of the trabecular meshwork after selective laser trabeculoplasty and low power argon laser trabeculoplasty," Lasers Surg. Med. **33**(3), 204–208 (2003).
28. J. R. SooHoo, L. K. Seibold, D. A. Ammar, and M. Y. Kahook, "Ultrastructural changes in human trabecular meshwork tissue after laser trabeculoplasty," J. Ophthalmol. **2015**, 1–5 (2015).
29. J. A. Alvarado, L. J. Katz, S. Trivedi, and A. S. Shifera, "Monocyte Modulation of Aqueous Outflow and Recruitment to the Trabecular Meshwork Following Selective Laser Trabeculoplasty," Arch. Ophthalmol. **128**(6), 731–737 (2010).
30. R. Bruen, M. R. Lesk, and P. Harasymowycz, "Baseline Factors Predictive of SLT Response: A Prospective Study," J. Ophthalmol. **2012**, 1–5 (2012).
31. A. J. Welch and M. J. Van Gemert, Optical-Thermal Response of Laser-Irradiated Tissue (Springer, 2011), Vol. 2.
32. "Laser-Tissue Interactions | SpringerLink," https://link.springer.com/book/10.1007%2F978-3-030-11917-1.
33. P. Arany, "Photobiomodulation therapy: Easy to do, but difficult to get right," Laser Focus World **55**, 22–24 (2019).
34. A. N. Kulikov, D. S. Maltsev, A. A. Kazak, and M. A. Burnasheva, "Anterior chamber particles are associated with reduction of intraocular pressure after selective laser trabeculoplasty," Br J Ophthalmol bjophthalmol **2019**, 315445 (2020).
35. N. Geffen, S. Ofir, A. Belkin, F. Segev, Y. Barkana, A. Kaplan Messas, E. I. Assia, and M. Belkin, "Transscleral Selective Laser Trabeculoplasty Without a Gonioscopy Lens:," J Glaucoma **26**(3), 201–207 (2017).
36. P. Li, L. An, G. Lan, M. Johnstone, D. S. Malchow, and R. K. Wang, "Extended imaging depth to 12 mm for 1050-nm spectral domain optical coherence tomography for imaging the whole anterior segment of the human eye at 120-kHz A-scan rate," J. Biomed. Opt. **18**(1), 016012 (2013).
37. A. Mohamed, D. Nankivil, V. Pesala, and M. Taneja, "The precision of ophthalmic biometry using calipers," Can. J. Ophthalmol. **48**(6), 506–511 (2013).
38. T. Kohnen, M. C. Thomala, M. Cichocki, and A. Strenger, "Internal anterior chamber diameter using optical coherence tomography compared with white-to-white distances using automated measurements," J. Cataract Refractive Surg. **32**(11), 1809–1813 (2006).
39. J. A. Goldsmith, Y. Li, M. R. Chalita, V. Westfall, C. Patel, A. M. Rollins, J. Izatt, and D. Huang, "Anterior Chamber Width Measurement by Optical Coherence Tomography," Invest. Ophthalmol. Vis. Sci. **44**, 3603 (2003).
40. T. Kasuga, Y.-C. Chen, Y. Hiratsuka, A. Murakami, M. Bloomer, and S. C. Lin, "Trabecular Meshwork Length In Men And Women Using Histological Specimen," Invest. Ophthalmol. Visual Sci. **53**, 3235 (2012).
41. L. Xu, R.-J. Yu, X.-M. Ding, M. Li, Y. Wu, L. Zhu, D. Chen, C. Peng, C.-J. Zeng, and W.-Y. Guo, "Efficacy of low-energy selective laser trabeculoplasty on the treatment of primary open angle glaucoma," Int J Ophthalmol **12**(9), 1432–1437 (2019).
42. K. Bliedtner, E. Seifert, and R. Brinkmann, "Towards Automatically Controlled Dosing for Selective Laser Trabeculoplasty," Trans. Vis. Sci. Tech. 8(6), 24 (2019).
43. A. J. Bron, "Wolff's Anatomy of the Eye and Orbit," (1997).
44. A. Vogel, C. Dlugos, R. Nuffer, and R. Birngruber, "Optical properties of human sclera, and their consequences for transscleral laser applications," Lasers Surg. Med. **11**(4), 331–340 (1991).
45. A. N. Bashkatov, E. A. Genina, A. Elina, V. I. Kochubey, T. G. Kamenskikh, and V. V. Tuchin, "Absorption and scattering properties of human eye sclera," *Saratov Fall Meeting* (2011).
46. Z. S. Sacks, R. M. Kurtz, T. Juhasz, and G. A. Mourou, "Femtosecond subsurface photodisruption in scattering human tissues using long infrared wavelengths," in *Saratov Fall Meeting 2000: Optical Technologies in Biophysics and Medicine II* (International Society for Optics and Photonics, 2001), Vol. 4241, pp. 98–111.
47. Z. S. Sacks, R. M. Kurtz, R. Fenn, F. H. Loesel, G. A. Mourou, and T. Juhasz, "Laser spot size as a function of tissue depth and laser wavelength in human sclera," in Applications of Ultrashort-Pulse Lasers in Medicine and Biology (International Society for Optics and Photonics, 1998), Vol. 3255, pp. 67–76.
48. Z. S. Sacks, D. L. Craig, R. M. Kurtz, T. Juhasz, and G. A. Mourou, "Spatially resolved transmission of highly focused beams through the cornea and sclera between 1400 and 1800nm," in *Saratov Fall Meeting '98: Light Scattering Technologies for Mechanics, Biomedicine, and Material Science* (International Society for Optics and Photonics, 1999), Vol. 3726, pp. 522–527.
49. Z. S. Sacks, R. M. Kurtz, T. Juhasz, and G. A. Mourou, "High precision subsurface photodisruption in human sclera," J. Biomed. Opt. **7**(3), 442–451 (2002).
50. D. Marti, R. N. Aasbjerg, P. E. Andersen, and A. K. Hansen, "MCmatlab: an open-source, user-friendly, MATLAB-integrated three-dimensional Monte Carlo light transport solver with heat diffusion and tissue damage," J. Biomed. Opt. **23**(12), 1 (2018).
51. M. Nagar, A. Ogunyomade, D. P. S. O'brart, F. Howes, and J. Marshall, "A randomised, prospective study comparing selective laser trabeculoplasty with latanoprost for the control of intraocular pressure in ocular hypertension and open angle glaucoma," Br. J. Ophthalmol. **89**(11), 1413–1417 (2005).
52. M. Nagar, E. Luhishi, and N. Shah, "Intraocular pressure control and fluctuation: the effect of treatment with selective laser trabeculoplasty," Br. J. Ophthalmol. **93**(4), 497–501 (2009).
53. C. L. Ho, J. S. M. Lai, M. V. Aquino, P. Rojanapongpun, H. T. Wong, M. C. Aquino, Y. Gerber, M. Belkin, and Y. Barkana, "Selective Laser Trabeculoplasty for Primary Angle Closure With Persistently Elevated Intraocular Pressure After Iridotomy," J Glaucoma **18**(7), 563–566 (2009).

Biomedical Optics EXPRESS

54. A. Garcés Fernández, I. Piloto Díaz, M. Miqueli Rodríguez, F. Pérez, A. Maurin, O. Carmona Pérez, and L. Peña López, "Trabeculoplastia selectiva con láser en glaucoma primario de ángulo cerrado," Revista Cubana de Oftalmología **23**, 27–37 (2010).
55. S. Raj, B. Tigari, T. T. Faisal, N. Gautam, S. Kaushik, P. Ichhpujani, S. S. Pandav, and J. Ram, "Efficacy of selective laser trabeculoplasty in primary angle closure disease," Eye **32**(11), 1710–1716 (2018).
56. A. Narayanaswamy, C. K. Leung, D. V. Istiantoro, S. A. Perera, C.-L. Ho, M. E. Nongpiur, M. Baskaran, H. M. Htoon, T. T. Wong, and D. Goh, "Efficacy of selective laser trabeculoplasty in primary angle-closure glaucoma: a randomized clinical trial," JAMA Ophthalmol. **133**(2), 206–212 (2015).
57. N. I. Kurysheva and L. V. Lepeshkina, "Selective Laser Trabeculoplasty Protects Glaucoma Progression in the Initial Primary Open-Angle Glaucoma and Angle-Closure Glaucoma after Laser Peripheral Iridotomy in the Long Term," BioMed Res. Int. **2019**, 1–10 (2019).
58. L. Ali Aljasim, O. Owaidhah, and D. P. Edward, "Selective laser trabeculoplasty in primary angle-closure glaucoma after laser peripheral iridotomy: a case-control study," J Glaucoma **25**(3), e253–e258 (2016).
59. N. I. Kurysheva, L. V. Lepeshkina, and E. O. Shatalova, "Predictors of Outcome in Selective Laser Trabeculoplasty: A Long-term Observation Study in Primary Angle-closure Glaucoma After Laser Peripheral Iridotomy Compared With Primary Open-angle Glaucoma," J Glaucoma **27**(10), 880–886 (2018).
60. M. A. Latina and C. Park, "Selective targeting of trabecular meshwork cells: in vitro studies of pulsed and CW laser interactions," Exp. Eye Res. **60**(4), 359–371 (1995).
61. M. F. Lieberman, N. G. Congdon, and M. He, "The value of tests in the diagnosis and management of glaucoma," Am. J. Ophthalmol. **152**(6), 889–899.e1 (2011).
62. L. Liu, "Australia and New Zealand survey of glaucoma practice patterns," Clin. Exp. Ophthalmol. **36**(1), 19–25 (2008).
63. "Market Scope. 2018 Glaucoma Surgical Device Report. Market Scope (R), LLC," (n.d.).
64. I. E. Commission, "IEC 60825–1: 2014. Safety of laser products—Part 1: Equipment classification and requirements," *IEC, Geneva* 3 (2014).
65. S. Arba-Mosquera and I. M. Aslanides, "Analysis of the effects of Eye-Tracker performance on the pulse positioning errors during refractive surgery," J. Optom. **5**(1), 31–37 (2012).
66. G. K. Bigley, "Headache," in Clinical Methods: The History, Physical, and Laboratory Examinations, H. K. Walker, W. D. Hall, and J. W. Hurst, eds., 3rd ed. (Butterworths, 1990).
67. K. Yee, "Active Eye Tracking for Excimer Laser Refractive Surgery," in Aberration-Free Refractive Surgery: New Frontiers in Vision, J. F. Bille, C. F. H. Harner, and F. F. Loesel, eds. (Springer, 2004), pp. 125–140.
68. M. D. Ober, M. Kernt, M. A. Cortes, and I. Kozak, "Time required for navigated macular laser photocoagulation treatment with the Navilas®," Graefes Arch Clin Exp Ophthalmol **251**(4), 1049–1053 (2013).